Hindawi Publishing Corporation
EURASIP Journal on Wireless Communications and Networking
Volume 2010, Article ID 873070, 12 pages
doi:10.1155/2010/873070

Research Article

A Propagation Environment Modeling in Foliage

Jing Liang,[1] Qilian Liang,[1] and Sherwood W. Samn[2]

[1] *Department of Electrical Engineering, University of Texas at Arlington, Arlington, TX 76019-0016, USA*
[2] *Air Force Research Laboratory/HEX, Brooks City Base, San Antonio, TX 78235, USA*

Correspondence should be addressed to Jing Liang, jliang@wcn.uta.edu

Received 16 September 2009; Accepted 22 January 2010

Academic Editor: Xiuzhen (Susan) Cheng

Foliage clutter, which can be very large and mask targets in backscattered signals, is a crucial factor that degrades the performance of target detection, tracking, and recognition. Previous literature has intensively investigated land clutter and sea clutter, whereas foliage clutter is still an open-research area. In this paper, we propose that foliage clutter should be more accurately described by a log-logistic model. On a basis of pragmatic data collected by ultra-wideband (UWB) radars, we analyze two different datasets by means of maximum likelihood (ML) parameter estimation as well as the root mean square error (RMSE) performance. We not only investigate log-logistic model, but also compare it with other popular clutter models, namely, log-normal, Weibull, and Nakagami. It shows that the log-logistic model achieves the smallest standard deviation (STD) error in parameter estimation, as well as the best goodness-of-fit and smallest RMSE for both poor and good foliage clutter signals.

1. Introduction and Motivation

Detection and identification of military equipment in a strong clutter background, such as foliage, soil cover, or building has been a long-standing subject of intensive study. It is believed that solving the target detection through foliage environment will significantly benefit sense-through-wall and many other subsurface sensing problems. However, to this date, the detection of foliage-covered targets with satisfied performances is still a challenging issue. Recent investigations in environment behavior of tree canopies have shown that both signal backscattering and attenuation are significantly influenced by tree architecture [1]. Therefore using the return signal from foliage to establish the clutter model that accounts for environment effects is of great importance for the sensing-through-foliage radar detection.

Clutter is a term used to define all unwanted echoes from natural environment [2]. The nature of clutter may necessarily vary on a basis of different applications and radar parameters. Most previous studies have investigated land clutter or sea clutter, and some conclusions have been reached. For example, log-normal, Weibull, and K-distributions have been proven to be better suited for the clutter description other than Rayleigh and Rician models in high-resolution radar systems. Fred did statistical comparisons and found that sea clutter at low-grazing angles and high range resolution is spiky based on the data measured from various sites in Kauai and Hawaii [3]. David generalized radar clutter models using noncentral chi-square density by allowing the noncentrality parameter to fluctuate according to the gamma distribution [4]. Furthermore, Leung et al. used a Neural-Network-based approach to predict the sea clutter model [5, 6].

However, as far as clutter modeling in forest is concerned, it is still of great interest and will be likely to take some time to reach any agreement. A team of researchers from MIT [7] and U. S. Army Research Laboratory (ARL) [8, 9] have measured ultra-wideband (UWB) backscatter signals in foliage for different polarizations and frequency ranges. The measurements show that the foliage clutter is impulsively corrupted with multipath fading, which leads to inaccuracy of the K-distributions description [10]. The US Air Force Office of Scientific Research (AFOSR) has conducted field measurement experiment concerning foliage penetration radar since 2004 and noted that metallic targets may be more easily identified with wideband than with narrowband signals.

In this investigation, we will apply ultra-wideband (UWB) radar to model the foliage clutter. UWB radar

emissions are at a relatively low frequency typically between 100 MHz and 3 GHz. Additionally, the fractional bandwidth of the signal is very large (greater than 0.2). Such a radar sensor has exceptional range resolution, as well as the ability to penetrate many common materials (e.g., walls). Law enforcement personnel have used UWB ground-penetrating radars (GPRs) for at least a decade. Like the GPR, sensing-through-foliage radar takes advantage of UWB's very fine resolution (time gating) and the low frequency of operation.

In our work, we investigate the log-logistic distribution (LLD) to model foliage clutter and illustrate the goodness-of-fit to real UWB clutter data. Additionally, we compare the goodness-of-fit of LLD with existing popular models, namely, log-normal, Weibull, and Nakagami by means of maximum likelihood estimation (MLE) and the root mean square error (RMSE). The result shows that log-logistic model provides the best fit to the foliage clutter. Our contribution is not only the new proposal on the foliage clutter model with detailed parameter estimation, but also providing the criteria and approaches based on which the statistical analysis is obtained. Further, based on LLD the theoretical study about the probability of detection as well as the probability of false alarm are discussed.

The rest of this paper is organized as follows. Section 2 provides a review on statistical models of log-logistic, log-normal, Weibull, and Nakagami, and discusses their applicability for foliage clutter modeling. Section 3 summarizes the measurement and the two sets of clutter data that are used in this paper. Section 4 discusses estimation on parameters and the goodness-of-fit for log-logistic, log-normal, Weibull and Nakagami models, respectively. Section 5 analyzes the performance of radar detection in the presence of foliage clutter. Finally, Section 6 concludes this paper and describes some future research topics.

2. Clutter Models

Many radar clutter models have been proposed in terms of distinct statistical distributions; most of which describe the characteristics of clutter amplitude or power. Before detailed analysis on our measurement, we would like to discuss the properties and applicability of log-logistic, log-normal, Weibull, and Nakagami statistic distributions, which are designated as "curve-fit" models in Section 4, since they are more likely to provide good fit to our collections of pragmatic clutter data. Detailed explanations would be given in the following subsections.

2.1. Log-Logistic Model. Recently Log-logistic model has been applied in hydrological analysis. This distribution is a special case of Burr's type-XII distribution [11] as well as a special case of the kappa distribution proposed by Mielke andJohnson [12]. Lee et al. employed the log-logistic distribution (LLD) for frequency analysis of multiyear drought durations [13], whereas Shoukri et al. employed LLD to analyze extensive Canadian precipitation data [14], and Narda and Malik used LLD to develop a model of root growth and water uptake in wheat [15]. In spite of its intensive application in precipitation and stream-flow data, the log-logistic distribution (LLD) [16] statistical model, to the best of our knowledge, has never been applied to radar foliage clutter. The motivation for considering log-logistic model is based on its higher kurtosis and longer tails, as well as its probability density function (PDF) similarity to log-normal and Weibull distributions. It is intended to be employed to estimate how well the model matches our collected foliage clutter statistics.

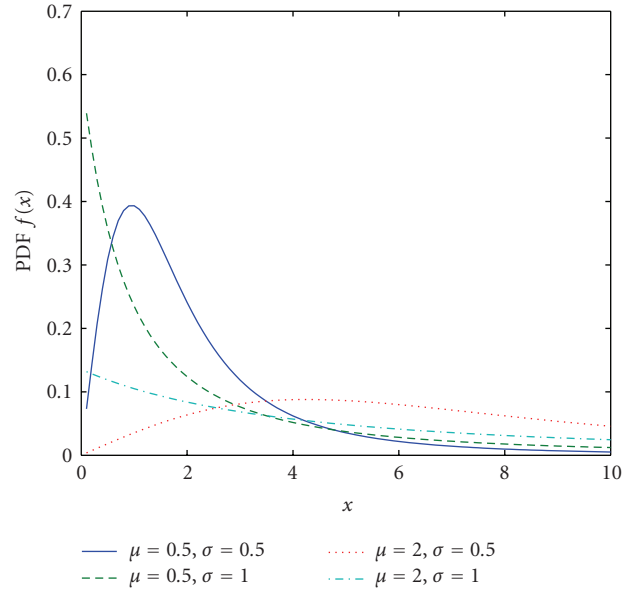

Figure 1: Log-logistic distribution PDF for $\mu = 0.5$ and $\sigma = 0.5$, $\mu = 0.5$ and $\sigma = 1$, $\mu = 2$ and $\sigma = 0.5$, $\mu = 2$ and $\sigma = 1$.

Here we apply the two-parameter distribution with parameters μ and σ. The PDF for this distribution is given by

$$f(x) = \frac{e^{((\ln x-\mu)/\sigma)}}{\sigma x\left(1+e^{((\ln x-\mu)/\sigma)}\right)^2}, \quad x > 0, \sigma > 0, \tag{1}$$

where μ is a scale parameter and σ is a shape parameter. The mean of the LLD is

$$E\{x\} = e^{\mu}\Gamma(1+\sigma)\Gamma(1-\sigma). \tag{2}$$

The variance is given by

$$\mathrm{Var}\{x\} = e^{2\mu}\left\{\Gamma(1+2\sigma)\Gamma(1-2\sigma) - [\Gamma(1+\sigma)\Gamma(1-\sigma)]^2\right\}, \tag{3}$$

while the moment of order k is

$$E\left\{x^k\right\} = \sigma e^{\mu}B(k\sigma, 1-k\sigma), \quad k < \frac{1}{\sigma}, \tag{4}$$

where

$$B(m,n) = \int_0^1 x^{m-1}(1-x)^{n-1}dx. \tag{5}$$

The PDFs for LLD for selected μ's and σ's are illustrated in Figure 1.

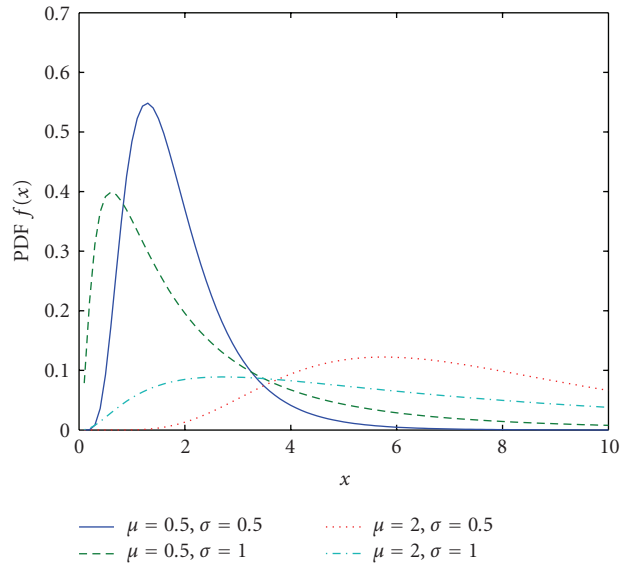

Figure 2: Log-normal distribution PDF for $\mu = 0.5$ and $\sigma = 0.5$, $\mu = 0.5$ and $\sigma = 1$, $\mu = 2$ and $\sigma = 0.5$, $\mu = 2$ and $\sigma = 1$.

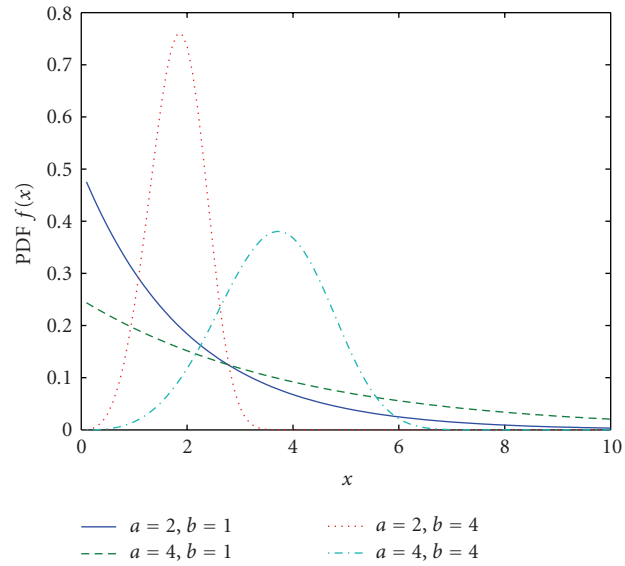

Figure 3: Weibull distribution PDF for $a = 2$ and $b = 1$, $a = 4$ and $b = 1$, $a = 2$ and $b = 4$, $a = 4$ and $b = 4$.

2.2. Log-Normal Model. The log-normal distribution is most frequently used when the radar sees land clutter [17] or sea clutter [18] at low-grazing angles (≤5 degrees) since log-normal has a long tail. However, it has been reported that the log-normal model tends to overestimate the dynamic range of the real clutter distribution [19]. Furthermore, whether it is applicable to model foliage clutter still requires detailed analysis.

The log-normal distribution [20] is also a two-parameter distribution with parameters μ and σ. The PDF for this distribution is given by

$$f(x) = \frac{1}{x\sigma\sqrt{2\pi}} e^{-(\ln x - \mu)^2/2\sigma^2}, \quad x > 0, \sigma > 0, \tag{6}$$

where μ is a scale parameter and σ is a shape parameter. The mean, variance, and the moment of order k are given, respectively, by

$$\begin{aligned} E\{x\} &= e^{\mu+(\sigma^2/2)}, \\ \mathrm{Var}\{x\} &= \left(e^{\sigma^2} - 1\right) e^{2\mu+\sigma^2}, \\ E\left\{x^k\right\} &= e^{k\mu+((k^2\sigma^2)/2)}. \end{aligned} \tag{7}$$

The PDFs for selected μ's and σ's for log-normal distribution are shown in Figure 2.

2.3. Weibull Model. The Weibull distribution, which is named after Waloddi Weibull, can be made to fit clutter measurements that lie between the Rayleigh and log-normal distribution [21]. It has been applied to land clutter [22, 23], sea clutter [24, 25] and weather clutter [26]. However, in very spiky sea and foliage clutter, the description of the clutter statistics provided by Weibull distributions may not always be sufficiently accurate [27].

The Weibull distribution is also a two-parameter distribution with parameters a and b. The PDF for this distribution is given by

$$f(x) = ba^{-b}x^{b-1}e^{-(x/a)^b}, \quad x > 0, a > 0, b > 0, \tag{8}$$

where b is the shape parameter and a is the scale parameter. The mean, variance, and the moment of order k are given, respectively, by

$$\begin{aligned} E\{x\} &= a\Gamma\left(1 + \frac{1}{b}\right), \\ \mathrm{Var}\{x\} &= a^2\left\{\Gamma\left(1 + \frac{2}{b}\right) - \left[\Gamma\left(1 + \frac{1}{b}\right)\right]^2\right\}, \\ E\left\{x^k\right\} &= a^k\Gamma\left(1 + \frac{k}{b}\right). \end{aligned} \tag{9}$$

The PDFs for selected a's and b's for Weibull distribution are shown in Figure 3.

2.4. Nakagami Model. In the foliage penetration setting, the target returns suffer from multipath effects corrupted with fading. As Nakagami distribution is used to model scattered fading signals that reach a receiver by multiple paths, it is natural to investigate how well it fits the foliage clutter statistics.

The PDF for Nakagami distribution is given by

$$f(x) = 2\left(\frac{\mu}{\omega}\right)^{\mu} \frac{1}{\Gamma(\mu)} x^{(2\mu-1)} e^{-(\mu/\omega)x^2}, \quad x > 0, \omega > 0, \tag{10}$$

where μ is the shape parameter and ω is the scale parameter.

The mean, variance, and the moment of order k of Nakagami distribution are given, respectively by

$$E\{x\} = \frac{\Gamma(\mu + (1/2))}{\Gamma(\mu)}\left(\frac{\omega}{\mu}\right)^{1/2},$$
$$\mathrm{Var}\{x\} = \omega\left[1 - \frac{1}{\mu}\left(\frac{\Gamma(\mu + (1/2))}{\Gamma(\mu)}\right)^{2}\right], \quad (11)$$
$$E\left\{x^{k}\right\} = \frac{\Gamma(\mu + (k/2))}{\Gamma(\mu)}\left(\frac{\omega}{\mu}\right)^{k/2}.$$

The PDFs for selected μ's and ω's for the Nakagami distribution are illustrated in Figure 4.

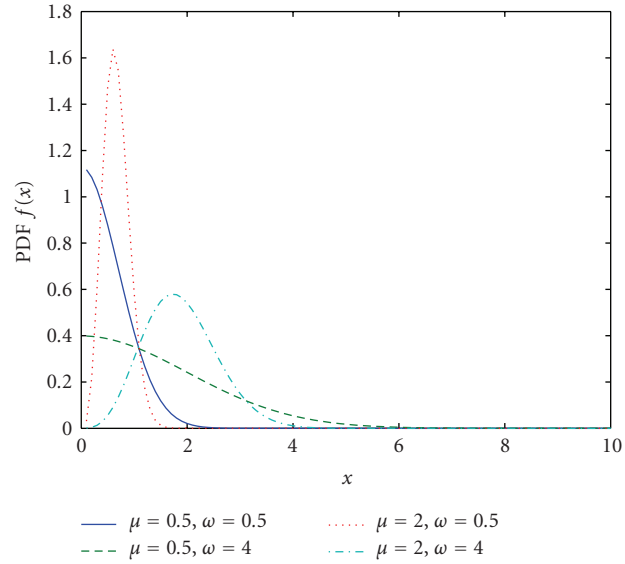

Figure 4: Nakagami distribution PDF for $\mu = 0.5$ and $\omega = 0.5$, $\mu = 0.5$ and $\omega = 4$, $\mu = 2$ and $\omega = 0.5$, $\mu = 2$ and $\omega = 4$.

3. Experiment Setup and Data Collection

The foliage penetration measurement effort began in August 2005 and continued through December 2005. Working in August through the fall of 2005, the foliage measured included late summer foliage and fall and early winter foliage. Late summer foliage, because of the limited rainfall, involved foliage with decreased water content. Late fall and winter measurements involved largely defoliated but dense forest. A picture of experiment site is shown in Figure 5.

The principle pieces of equipment are

(i) Dual antenna mounting stand,

(ii) Two antennas,

(iii) A trihedral reflector target,

(iv) Barth pulse source (Barth Electronics, Inc. model 732 GL) for UWB,

(v) Tektronix model 7704 B oscilloscope,

(vi) Rack system,

(vii) HP signal Generator,

(viii) IBM laptop,

(ix) Custom RF switch and power supply,

(x) Weather shield (small hut).

Figure 5: A picture of foliage.

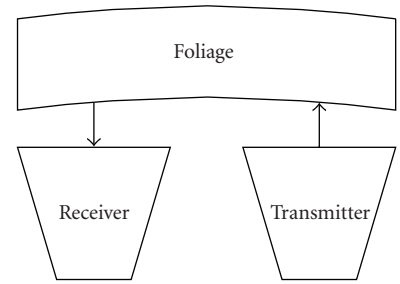

Figure 6: Illustration for the experimental radar antennas.

A bistatic UWB radar (individual transmit and receive antennas) was used (see Figure 6) as it was believed that circulators did not exist for wideband signals at that time. The foliage clutter was a round trip distance of 600 feet from the bistatic antennas (300 feet one way).

An 18-foot distance between antennas was chosen to reduce the signal coupling between transmitter and the receiver [28]. The radar was constructed on a seven-ton man lift, which had a total lifting capacity of 450 kG. The limit of the lifting capacity was reached during the experiment as essentially the entire measuring apparatus was placed on the lift (as shown in Figure 7). Throughout this work, a Barth pulse source (Barth Electronics, Inc., model 732 GL) was used. The pulse generator uses a coaxial reed switch to discharge a charge line for a very fast rise-time pulse outputs. The model 732 pulse generator provides pulses of less than 50 picoseconds (ps) rise time, with amplitude from 150 V to greater than 2 kV into any load impedance through a 50 ohm coaxial line. The generator is capable of producing pulses with a minimum width of 750 ps and a maximum of 1 microsecond. This output pulse width is determined by charge line length for rectangular pulses, or by capacitors for 1/e decay pulses.

For the return data we used in this paper, each sample is spaced at 50 picoseconds interval, and 16.000 samples were collected for each collection for a total time duration

Figure 7: This figure shows the lift with the experiment. The antennas are at the far end of the lift from the viewer under the roof that was built to shield the equipment from the elements. This picture was taken in September with the foliage largely still present. The cables coming from the lift are a ground cable to an earth ground and one of 4 tethers used in windy conditions.

of 0.8 microseconds at a rate of approximately 20 Hz. We considered two sets of data from this experiment. Initially, the Barth pulse source was operated at lower amplitude and 35 pulses of clutter signals were obtained at each site but different time. These pulses have been averaged to remove the random noise. Data have been collected from 10 different sites. one collection of transmitted pulse and received backscattering are shown in Figures 8(a) and 8(b), respectively. The unit of clutter amplitude in this paper is "V". Although pulse-to-pulse variability was noted for collections of received echoes, the decay profiles of returned signals are quite similar. These data are referred to as dataset I.

Later, additional improvements were made in the measurement procedure, including the improved isolation of transmit and receive antennas, the addition of a log-periodic antenna (Antenna Research Associates LPC-2010-C) as a transmit antenna, and the EMCO ridged waveguide horn (Microwave horn, EMCO 3106). Echoes for dataset II were collected using this higher-amplitude transmitted pulses. Two collections at different site with 100 pulses average have been obtained; one of which is shown in Figure 8(c). To make them clearer to readers, we provide expanded views of received traces from samples 10.000 to 12.000 in Figure 9.

4. Statistical Analysis of the Foliage Clutter

4.1. Maximum Likelihood Estimation. Using the collected clutter data mentioned above, we apply Maximum Likelihood Estimation (MLE) approach to estimate the parameters of the log-logistic, log-normal, Weibull, and Nakagami models. MLE is often used when the sample data are known and parameters of the underlying probability distribution are to be estimated [29, 30]. It is generalized as follows.

Let $y_1, y_2, \ldots, y_N$ be N independent samples drawn from a random variable $\mathbf{Y}$ with m parameters $\theta_1, \theta_2, \ldots, \theta_m$, where $\theta_i \in \theta$, then the likelihood function expressed as a function of θ conditional on $\mathbf{Y}$ is

$$L_N(\mathbf{Y} \mid \theta) = \prod_{k=1}^{N} f_{Y|\theta}(y_k \mid \theta_1, \theta_2, \ldots, \theta_m). \tag{12}$$

The maximum likelihood estimate of θ_1, θ_2,..., θ_m is the set of values $\hat{\theta}_1, \hat{\theta}_2, \ldots, \hat{\theta}_m$ that maximize the likelihood function $L_N(\mathbf{Y} \mid \theta)$.

As the logarithmic function is monotonically increasing, maximizing $L_N(\mathbf{Y} \mid \theta)$ is equivalent to maximizing $\ln(L_N(\mathbf{Y} \mid \theta))$. Hence, it can be shown that a necessary but not sufficient condition to obtain the ML estimate $\hat{\theta}$ is to solve the likelihood equation

$$\frac{\partial}{\partial \theta} \ln(L_N(\mathbf{Y} \mid \theta)) = 0. \tag{13}$$

Note that the amplitude of foliage clutter faded with the increase of sample time. Even at the same sample, it varies for different collections. In order to better analyze its randomness, we studied each collection. Using the collected clutter radar mentioned above, we apply MLE to obtain $\hat{\mu}$ and $\hat{\sigma}$ for log-logistic, $\hat{\mu}$ and $\hat{\sigma}$ for the log-normal, $\hat{a}$ and $\hat{b}$ for the Weibull, and $\hat{\mu}$ and $\hat{\omega}$ for the Nakagami. The estimation results for dataset I are listed in Table 1. We also explore the standard deviation (STD) error of each parameter. These descriptions are shown in Table 1 in the form of ε_x, where x denotes different parameter for each model. We also calculate the average values of estimated parameters and their STD errors in Table 2.

From Tables 1 and 2, it can be easily seen that STD errors for log-logistic and log-normal parameters are less than 0.02 and the estimated parameters for these two models vary little from data to data compared to parameters of Weibull and Nakagami. It is obvious that log-logistic model provides the smallest STD error for all the 10 collections compared to log-normal. Although accurate shape parameter estimation can be achieved by both Weibull and Nakagami models, their scale parameters are not acceptable.

The estimation results for dataset II are shown in Table 3. Due to the improvement on this set of signal, STD error for log-logistic and log-normal parameters have been reduced compared to those in dataset I. However, for Weibull and Nakagami, it is a different case, which implies that log-logistic and log-normal are much more accurate to model foliage clutter.

In view of smaller error in parameter estimation, log-logistic model fits the collected data best compared to log-normal, Weibull, and Nakagami. Log-normal model is also acceptable.

Table 1: Estimated parameters for dataset I.

PDF	Log-Logistic	Log-normal	Weibull	Nakagami
Data 1	$\hat{\mu} = 7.24161$	$\hat{\mu} = 7.0455$	$\hat{a} = 2975.33$	$\hat{\mu} = 0.177062$
	$\hat{\sigma} = 1.06483$	$\hat{\sigma} = 2.20761$	$\hat{b} = 0.594979$	$\hat{\omega} = 9.09663e+007$
	$\varepsilon_\mu = 0.0141212$	$\varepsilon_\mu = 0.0174527$	$\varepsilon_a = 41.6157$	$\varepsilon_\mu = 0.00150615$
	$\varepsilon_\sigma = 0.00724181$	$\varepsilon_\sigma = 0.0123415$	$\varepsilon_b = 0.00356925$	$\varepsilon_\omega = 1.70907e+006$
Data 2	$\hat{\mu} = 6.9716$	$\hat{\mu} = 6.72573$	$\hat{a} = 2285.13$	$\hat{\mu} = 0.162375$
	$\hat{\sigma} = 1.2126$	$\hat{\sigma} = 2.33617$	$\hat{b} = 0.563747$	$\hat{\omega} = 7.4776e+007$
	$\varepsilon_\mu = 0.014747$	$\varepsilon_\mu = 0.0184691$	$\varepsilon_a = 33.7127$	$\varepsilon_\mu = 0.00137422$
	$\varepsilon_\sigma = 0.00773723$	$\varepsilon_\sigma = 0.0130602$	$\varepsilon_b = 0.00337485$	$\varepsilon_\omega = 1.46679e+006$
Data 3	$\hat{\mu} = 7.00554$	$\hat{\mu} = 6.76262$	$\hat{a} = 2341.52$	$\hat{\mu} = 0.164695$
	$\hat{\sigma} = 1.10741$	$\hat{\sigma} = 2.31258$	$\hat{b} = 0.57073$	$\hat{\omega} = 7.46366e+007$
	$\varepsilon_\mu = 0.0145728$	$\varepsilon_\mu = 0.0182825$	$\varepsilon_a = 34.1207$	$\varepsilon_\mu = 0.001395$
	$\varepsilon_\sigma = 0.0076303$	$\varepsilon_\sigma = 0.0129283$	$\varepsilon_b = 0.00341448$	$\varepsilon_\omega = 1.45459e+006$
Data 4	$\hat{\mu} = 7.03055$	$\hat{\mu} = 6.80711$	$\hat{a} = 2395.85$	$\hat{\mu} = 0.167391$
	$\hat{\sigma} = 1.07858$	$\hat{\sigma} = 2.25973$	$\hat{b} = 0.579381$	$\hat{\omega} = 7.4926e+007$
	$\varepsilon_\mu = 0.0142027$	$\varepsilon_\mu = 0.0178647$	$\varepsilon_a = 34.4066$	$\varepsilon_\mu = 0.0014916$
	$\varepsilon_\sigma = 0.00741556$	$\varepsilon_\sigma = 0.0126329$	$\varepsilon_b = 0.00345156$	$\varepsilon_\omega = 1.44727e+006$
Data 5	$\hat{\mu} = 7.16226$	$\hat{\mu} = 6.95712$	$\hat{a} = 2806.76$	$\hat{\mu} = 0.17112$
	$\hat{\sigma} = 1.10132$	$\hat{\sigma} = 2.26592$	$\hat{b} = 0.577823$	$\hat{\omega} = 9.03298e+007$
	$\varepsilon_\mu = 0.014605$	$\varepsilon_\mu = 0.0179137$	$\varepsilon_a = 40.4226$	$\varepsilon_\mu = 0.00145265$
	$\varepsilon_\sigma = 0.00750067$	$\varepsilon_\sigma = 0.0126675$	$\varepsilon_b = 0.00347389$	$\varepsilon_\omega = 1.72749e+006$
Data 6	$\hat{\mu} = 7.01527$	$\hat{\mu} = 6.77515$	$\hat{a} = 2360.33$	$\hat{\mu} = 0.165292$
	$\hat{\sigma} = 1.10123$	$\hat{\sigma} = 2.30286$	$\hat{b} = 0.572749$	$\hat{\omega} = 7.50824e+007$
	$\varepsilon_\mu = 0.0144902$	$\varepsilon_\mu = 0.0182057$	$\varepsilon_a = 34.2753$	$\varepsilon_\mu = 0.00140035$
	$\varepsilon_\sigma = 0.00758568$	$\varepsilon_\sigma = 0.012874$	$\varepsilon_b = 0.00342376$	$\varepsilon_\omega = 1.46145e+006$
Data 7	$\hat{\mu} = 7.14523$	$\hat{\mu} = 6.94201$	$\hat{a} = 2753.69$	$\hat{\mu} = 0.170964$
	$\hat{\sigma} = 1.09486$	$\hat{\sigma} = 2.25621$	$\hat{b} = 0.578948$	$\hat{\omega} = 8.80474e+007$
	$\varepsilon_\mu = 0.0145132$	$\varepsilon_\mu = 0.0178369$	$\varepsilon_a = 39.585$	$\varepsilon_\mu = 0.00145125$
	$\varepsilon_\sigma = 0.00745994$	$\varepsilon_\sigma = 0.0126132$	$\varepsilon_b = 0.00347442$	$\varepsilon_\omega = 1.68382e+006$
Data 8	$\hat{\mu} = 6.95411$	$\hat{\mu} = 6.71591$	$\hat{a} = 2250.66$	$\hat{\mu} = 0.162448$
	$\hat{\sigma} = 1.11486$	$\hat{\sigma} = 2.31898$	$\hat{b} = 0.564989$	$\hat{\omega} = 7.31436e+007$
	$\varepsilon_\mu = 0.0146774$	$\varepsilon_\mu = 0.0183331$	$\varepsilon_a = 33.1387$	$\varepsilon_\mu = 0.00137488$
	$\varepsilon_\sigma = 0.00768003$	$\varepsilon_\sigma = 0.0129641$	$\varepsilon_b = 0.0033763$	$\varepsilon_\omega = 1.4338e+006$
Data 9	$\hat{\mu} = 7.18561$	$\hat{\mu} = 6.9715$	$\hat{a} = 2840.72$	$\hat{\mu} = 0.172324$
	$\hat{\sigma} = 1.09854$	$\hat{\sigma} = 2.27088$	$\hat{b} = 0.581219$	$\hat{\omega} = 8.97304e+007$
	$\varepsilon_\mu = 0.0145483$	$\varepsilon_\mu = 0.0179529$	$\varepsilon_a = 40.6593$	$\varepsilon_\mu = 0.00146348$
	$\varepsilon_\sigma = 0.00749265$	$\varepsilon_\sigma = 0.0126952$	$\varepsilon_b = 0.0034984$	$\varepsilon_\omega = 1.70923e+006$
Data 10	$\hat{\mu} = 7.192$	$\hat{\mu} = 6.99196$	$\hat{a} = 2869.65$	$\hat{\mu} = 0.173572$
	$\hat{\sigma} = 1.0866$	$\hat{\sigma} = 2.23975$	$\hat{b} = 0.584803$	$\hat{\omega} = 9.01631e+007$
	$\varepsilon_\mu = 0.0144166$	$\varepsilon_\mu = 0.0177067$	$\varepsilon_a = 40.837$	$\varepsilon_\mu = 0.0014747$
	$\varepsilon_\sigma = 0.0073916$	$\varepsilon_\sigma = 0.0125211$	$\varepsilon_b = 0.00351294$	$\varepsilon_\omega = 1.71142e+006$

Table 2: Averaged estimated parameters for dataset I.

PDF	Log-Logistic	Log-normal	Weibull	Nakagami
Average	$\hat{\mu} = 7.0904$	$\hat{\mu} = 6.8695$	$\hat{a} = 2588$	$\hat{\mu} = 0.1687$
	$\hat{\sigma} = 1.1061$	$\hat{\sigma} = 2.2771$	$\hat{b} = 0.5769$	$\hat{\omega} = 8.218e+007$
	$\varepsilon_\mu = 0.0145$	$\varepsilon_\mu = 0.0180$	$\varepsilon_a = 37.4316$	$\varepsilon_\mu = 0.0014$
	$\varepsilon_\sigma = 0.0075$	$\varepsilon_\sigma = 0.0127$	$\varepsilon_b = 0.0035$	$\varepsilon_\omega = 1.4905e+006$

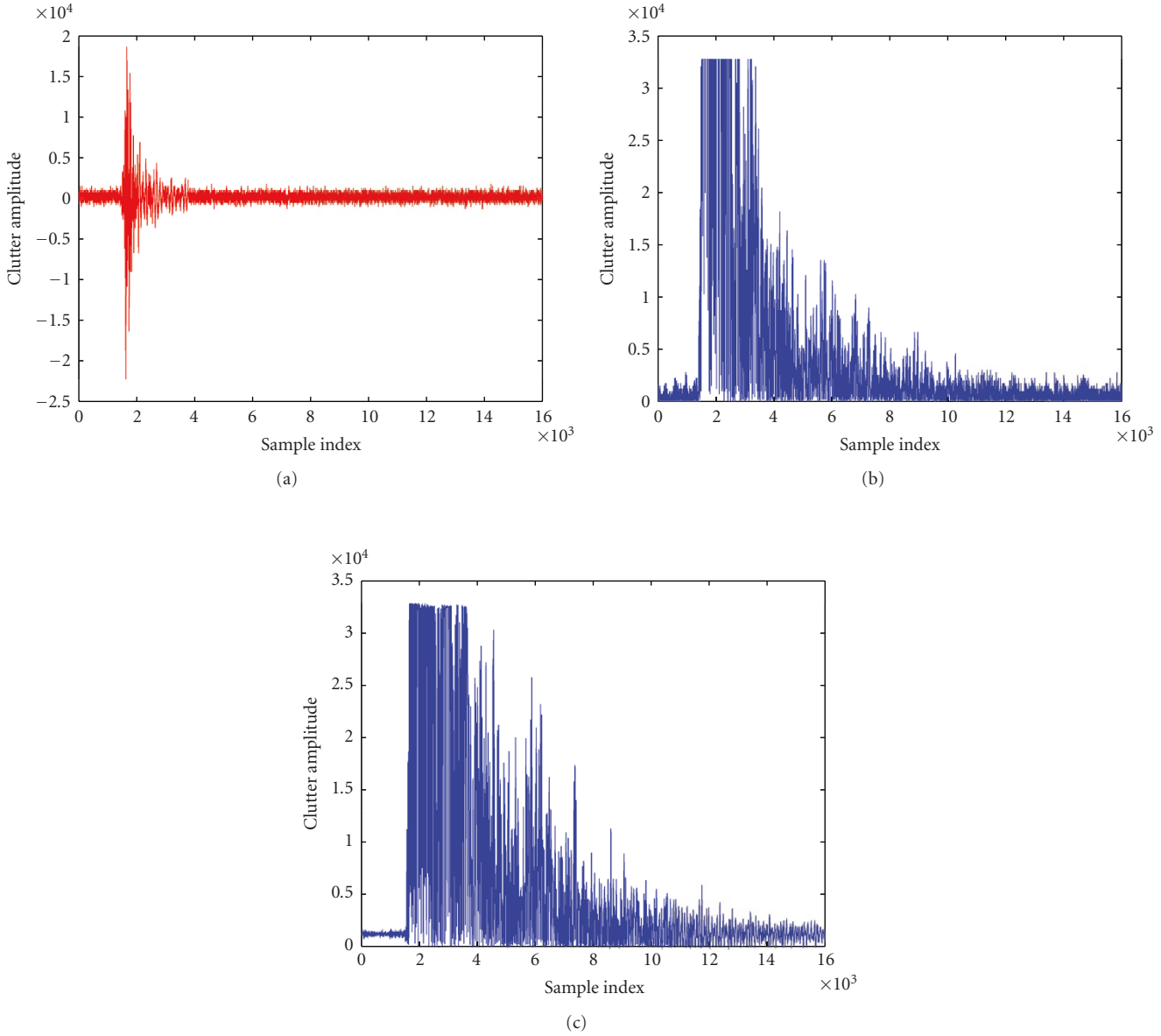

Figure 8: Clutter data: (a) transmitted pulse before antenna amplification, (b) an example of received echoes from dataset I, and (c) an example of received echoes from dataset II.

4.2. Goodness-of-Fit in Curve and RMSE. We may also observe the extent to which the PDF curve of the statistic model matches that of clutter data by calculating the averaged root mean square error (RMSE) for each dataset. Let i (i=1, 2, ..., n) be the sample index of clutter amplitude; c_i is the corresponding PDF value whereas $\hat{c}_i$ is the PDF value of the statistical model with estimated parameters by means of MLE. The RMSE is obtained by

$$\text{RMSE} = \frac{1}{k}\sum_{k}\sqrt{\frac{1}{n}\sum_{i=1}^{n}(c_i - \hat{c}_i)^2}. \tag{14}$$

Here we apply n =100 for each model and k is the number of data collections for each set.

In Figures 10 and 11, we use one collection from dataset I and II, respectively to illustrate the goodness-of-fit in curve. Also, we calculate the averaged RMSE of each model for both collected dataset I and II. The PDF of absolute amplitude of one collection of clutter data is presented by means of histogram bars. In Figure 10, it can be seen obviously that log-logistic model with MLE parameters provides the best goodness-of-fit compared to other models, since it provides the most suitable kurtosis, slope and tail. As for the maximum PDF value, the log-logistic is about 1×10^{-3}, while those of other models are over 1.2×10^{-3}. For the slope part, which connects the kurtosis and the tail, and is in the range from 0.1×10^4 to 0.5×10^4 by x axes, the log-logistic model provides the smallest skewness whereas Nakagami

Table 3: Estimated and averaged parameters for dataset ii.

PDF	Log-Logistic	Log-normal	Weibull	Nakagami
Data 1	$\hat{\mu} = 7.76868$	$\hat{\mu} = 7.79566$	$\hat{a} = 4901.07$	$\hat{\mu} = 0.239587$
	$\hat{\sigma} = 0.786511$	$\hat{\sigma} = 1.41771$	$\hat{b} = 0.743223$	$\hat{\omega} = 1.16839e+008$
	$\varepsilon_\mu = 0.0107792$	$\varepsilon_\mu = 0.011208$	$\varepsilon_a = 55.3011$	$\varepsilon_\mu = 0.00207912$
	$\varepsilon_\sigma = 0.00521601$	$\varepsilon_\sigma = 0.00792559$	$\varepsilon_b = 0.00434465$	$\varepsilon_\omega = 1.88719e+006$
Data 2	$\hat{\mu} = 7.78096$	$\hat{\mu} = 7.8046$	$\hat{a} = 4942.48$	$\hat{\mu} = 0.240593$
	$\hat{\sigma} = 0.787426$	$\hat{\sigma} = 1.41855$	$\hat{b} = 0.745233$	$\hat{\omega} = 1.17237e+008$
	$\varepsilon_\mu = 0.0107917$	$\varepsilon_\mu = 0.0112147$	$\varepsilon_a = 55.6114$	$\varepsilon_\mu = 0.00208848$
	$\varepsilon_\sigma = 0.0052213$	$\varepsilon_\sigma = 0.00793033$	$\varepsilon_b = 0.0043612$	$\varepsilon_\omega = 1.88953e+006$
Average	$\hat{\mu} = 7.7748$	$\hat{\mu} = 7.7881$	$\hat{a} = 4921.8$	$\hat{\mu} = 0.2401$
	$\hat{\sigma} = 0.7870$	$\hat{\sigma} = 1.4181$	$\hat{b} = 0.7442$	$\hat{\omega} = 1.1704 + 008$
	$\varepsilon_\mu = 0.0108$	$\varepsilon_\mu = 0.0112$	$\varepsilon_a = 55.4565$	$\varepsilon_\mu = 0.0021$
	$\varepsilon_\sigma = 0.0052$	$\varepsilon_\sigma = 0.0079$	$\varepsilon_b = 0.0044$	$\varepsilon_\omega = 1.8884 + 006$

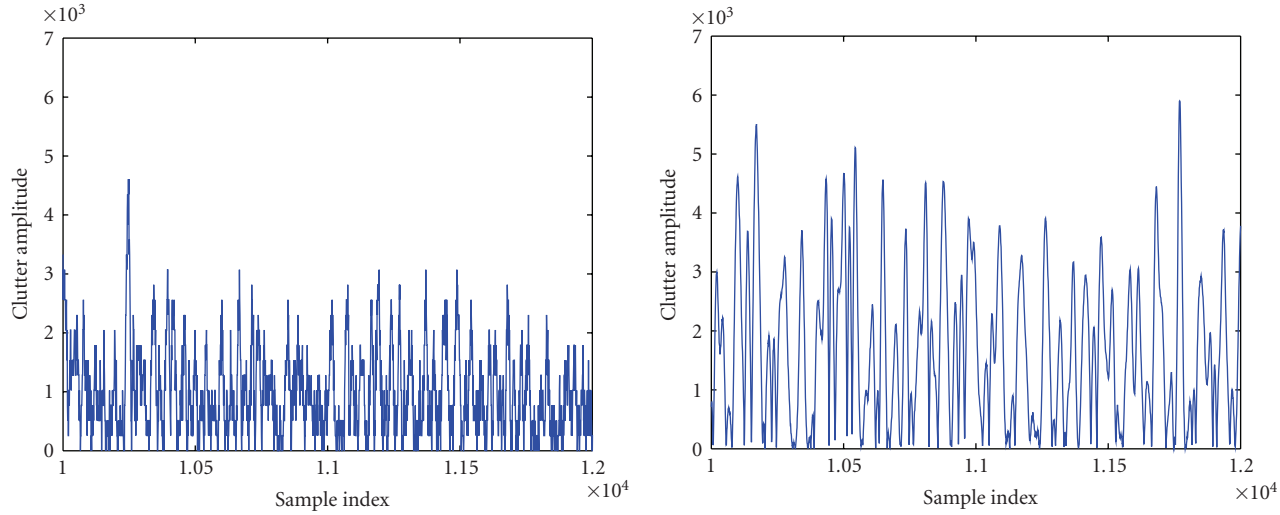

Figure 9: Expanded view from clutter samples 10.000 to 12.000 (a) from dataset I, and (b) from dataset II.

provides the largest. Examination of these tails shows that log-logistic and log-normal provide very similar-valued tails, while tails of the Weibull and the Nakagami are lager than the collected data. Meanwhile, we obtain that $\text{RMSE}_{\text{log-logistic}} = 2.5425\times10^{-5}$, $\text{RMSE}_{\text{log-normal}} = 3.2704\times10^{-5}$, $\text{RMSE}_{\text{Weibull}} = 3.7234 \times 10^{-5}$, and $\text{RMSE}_{\text{Nakagami}} = 5.4326 \times 10^{-5}$. This also illustrates that the log-logistic model is more accurate than the other three models.

Similarly, in Figure 11 histogram bars denote the PDF of the absolute amplitude of one collection of clutter data from set II. Compared to Figure 10, the log-logistic and the log-normal provide similar extent of goodness-of-fit. Weibull is worse since it cannot fit well in either kurtosis or tail, while Nakagami is the worst and unacceptable. Also, we obtain $\text{RMSE}_{\text{log-logistic}} = 2.739 \times 10^{-5}$, $\text{RMSE}_{\text{log-normal}} = 3.1866 \times 10^{-5}$, $\text{RMSE}_{\text{Weibull}} = 3.6361 \times 10^{-5}$, and $\text{RMSE}_{\text{Nakagami}} = 4.4045 \times 10^{-5}$. This illustrates that for clutter backscattering dataset II, the log-logistic model still fits the best.

5. Target Detection Performance

One of the primary goals for a radar is target detection; therefore based on clutter models that have been investigated in the previous sections, we apply a special case of the Bayesian criterion named Neyman-Parson criterion to analyze the target detection performance in the foliage environment.

If the received sample signal is R, then the two hypotheses are shown as follows.

$$H_0 : R = C + n,$$
$$H_1 : R = S + C + n, \tag{15}$$

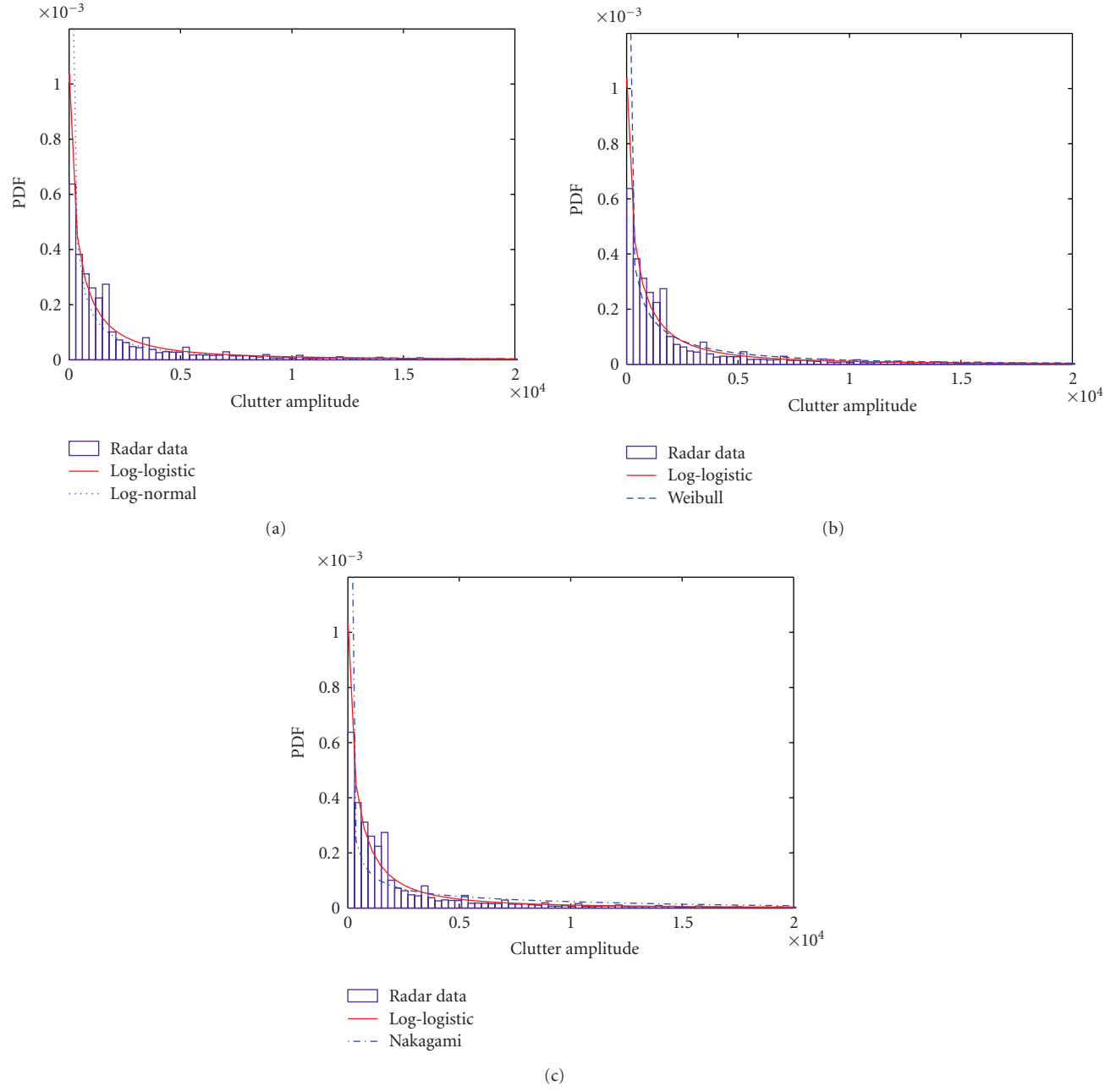

FIGURE 10: Clutter model comparison from dataset I: (a) log-logistic versus log-normal, (b) log-logistic versus Weibull, and (c) log-logistic versus Nakagami. $\text{RMSE}_{\text{log-logistic}} = 2.5425 \times 10^{-5}$, $\text{RMSE}_{\text{log-normal}} = 3.2704 \times 10^{-5}$, $\text{RMSE}_{\text{Weibull}} = 3.7234 \times 10^{-5}$, and $\text{RMSE}_{\text{Nakagami}} = 5.4326 \times 10^{-5}$.

where C and n represent the random variable of clutter and noise, respectively. C follows log-logistic model with both parameters μ and σ, and n is Gaussian noise with zero mean and variance ν^2. S is the target signal, which assumes to be a constant for simplicity.

Therefore $f(R \mid H_0)$ and $f(R \mid H_1)$ mean that

(i) $f(R \mid H_0)$ = PDF of R given that a target was not present,

(ii) $f(R \mid H_1)$ = PDF of R given that a target was present.

They can be denoted as follows.

$$f(R \mid H_0) = \int_0^\infty \frac{e^{(\ln r-\mu)/\sigma}}{\sigma r\left(1+e^{(\ln r-\mu)/\sigma}\right)^2} \times \frac{1}{\sqrt{2\pi}\nu} e^{-(R-r)^2/2\nu^2} dr, \tag{16}$$

$$f(R \mid H_1) = \int_0^\infty \frac{e^{((\ln(r-s)-\mu)/\sigma)}}{\sigma(r-s)\left(1+e^{((\ln(r-s)-\mu)/\sigma)}\right)^2} \times \frac{1}{\sqrt{2\pi}\nu} e^{-(R-s-r)^2/2\nu^2} dr. \tag{17}$$

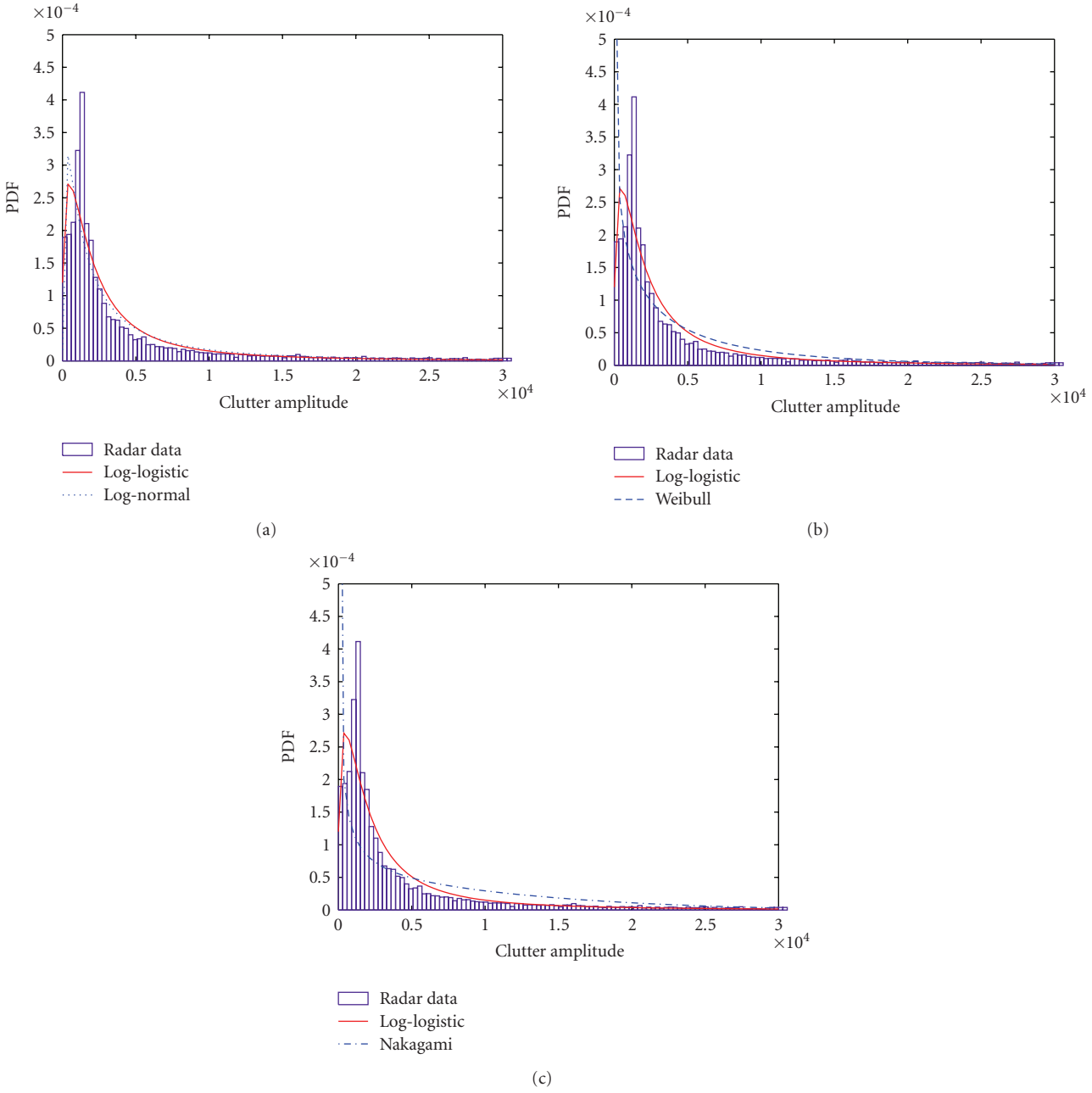

FIGURE 11: Clutter model comparison from dataset II: (a) log-Logistic versus log-normal, (b) log-logistic versus Weibull (c), and log-logistic versus Nakagami. $\text{RMSE}_{\text{log-logistic}} = 2.739 \times 10^{-5}$, $\text{RMSE}_{\text{log-normal}} = 3.1866 \times 10^{-5}$, $\text{RMSE}_{\text{Weibull}} = 3.6361 \times 10^{-5}$, and $\text{RMSE}_{\text{Nakagami}} = 4.4045 \times 10^{-5}$.

If the probability that a target was not present is $P(H_0)$ whereas the probability that a target was present is $P(H_1)$, then PDF of R is

$$f(R) = P(H_0)f(R \mid H_0) + P(H_1)f(R \mid H_1). \tag{18}$$

To decide whether there is a target or not, Neyman-Pearson detection rule is shown as

$$\frac{f(R \mid H_0)}{f(R \mid H_1)} \underset{H_1}{\overset{H_0}{\gtrless}} \frac{P(H_1)}{P(H_0)}. \tag{19}$$

In case of $P(H_1) = P(H_0)$, (20) is simplified as

$$f(R \mid H_0) \underset{H_1}{\overset{H_0}{\gtrless}} f(R \mid H_1), \tag{20}$$

which actually is

$$\frac{e^{[((s^2-2s(R-r))/2\gamma^2)+(\ln((r/r-s))/\sigma)]}}{(r/(r-s))\left[\left(1+e^{((\ln r-\mu)/\sigma)}\right)/\left(1+e^{((\ln(r-s)-\mu)/\sigma)}\right)\right]^2} \underset{H_1}{\overset{H_0}{\gtrless}} 1. \tag{21}$$

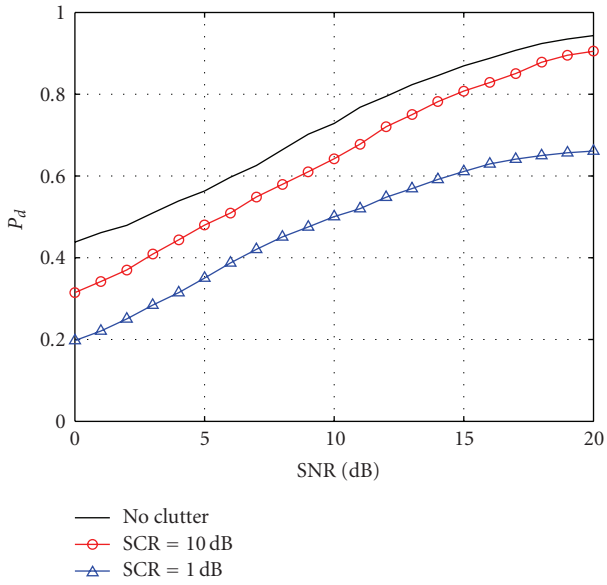

Figure 12: Probability of detection.

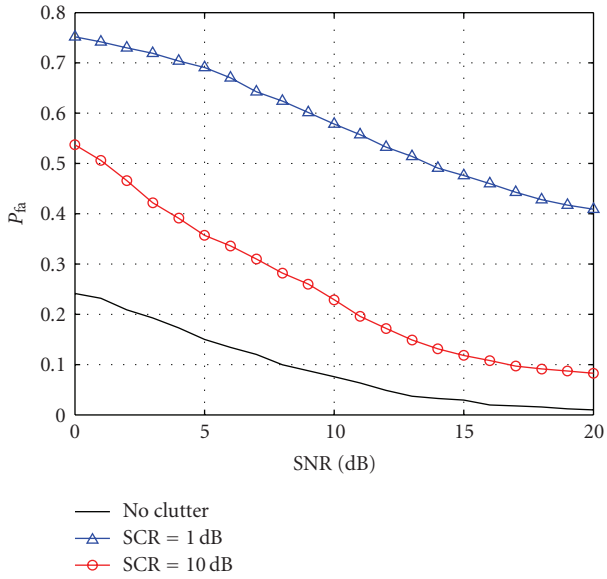

Figure 13: Probability of false alarm.

It is easy to obtain the decision threshold T in terms of the above function:

$$T = -\frac{\nu^2}{s}\ln\left[\frac{1+e^{((\ln r-\mu)/\sigma)}}{1+e^{((\ln(r-s)-\mu)/\sigma)}}\right]^2 + \frac{\nu^2[\ln(r/(r-s))-\sigma]}{s\sigma} + \frac{s}{2} + r. \tag{22}$$

Under hypothesis H_0, a false alarm occurs anytime $R > T$, therefore the probability of false alarm is

$$\begin{aligned} P_{\mathrm{FA}} &= \int_T^\infty f(R \mid H_0)dR \\ &= \frac{1}{\sqrt{2\pi}\sigma\nu}\int_T^\infty\int_0^\infty \frac{e^{[-((R-r)^2/2\nu^2)+((\ln r-\mu)/\sigma)]}}{\left(1+e^{((\ln r-\mu)/\sigma)}\right)^2 r}dr\,dR. \end{aligned} \tag{23}$$

Similarly, under hypothesis H_1, when $R > T$, the target is detectable. Therefore the probability of detection is

$$\begin{aligned} P_D &= \int_T^\infty f(R \mid H_1)dR, \\ &= \frac{1}{\sqrt{2\pi}\sigma\nu}\int_T^\infty\int_0^\infty \frac{e^{[-((R-r-s)^2/2\nu^2)+(\ln(r-s)-\mu)/\sigma]}}{\left(1+e^{((\ln(r-s)-\mu)/\sigma)}\right)^2 (r-s)}dr\,dR. \end{aligned} \tag{24}$$

Figure 12 shows the probability of detection for a fluctuating radar target using Monte Carlo simulation. The "no clutter" curve describes the situation when there are only radar echoes and noise. Swerling II model is applied for the detection [31]. "SCR" stands for signal-to-clutter ratio, where log-logistic clutter model is used, and "SNR" is the signal to noise ratio. These curves show that, no matter what SCR is, the clutter generally reduces the probability of detection. When SCR increases, the probability of detection will become more close to the value of "no clutter" case along with the increase of SNR. Similarly, Figure 13 illustrates the probability of false alarm, which shows that the clutter tremendously increase the probability of false alarm.

6. Conclusion

On a basis of two sets of foliage clutter data collected by a UWB radar, we show that it is more accurate to describe the amplitude of foliage clutter using log-logistic statistic model rather than log-normal, Weibull, or Nakagami. Log-normal is also acceptable. The goodness-of-fit for Weibull is worse whereas that of Nakagami is the worst. Our contribution is not only the new proposal on the foliage clutter model with detailed parameters, but also providing the criteria and approaches based on which the statistical analysis is obtained. Further, the theoretical study on the probability of detection and the probability of false alarm in the presence of log-logistic foliage clutter are discussed. Future research will investigate the characteristics of targets and the design of radar receivers for the log-logistic clutter so as to improve the performance of target detection, tracking and identification in foliage.

Acknowledgments

This work was supported in part by the U.S. Office of Naval Research under Grant N00014-07-1-0395 and Grant 00014-07-1-1024 and in part by the National Science Foundation under Grant CNS-0721515, Grant CNS-0831902, Grant CCF-0956438, and Grant CNS-0964713.

References

[1] M. L. Imhoff, "A theoretical analysis of the effect of forest structure on synthetic aperture radar backscatter and the remote sensing of biomass," *IEEE Transactions on Geoscience and Remote Sensing*, vol. 33, no. 2, pp. 341–352, 1995.

[2] M. I. Skolnik, *Introduction to Radar Systems*, McGraw-Hill, New York, NY, USA, 3rd edition, 2001.

[3] F. L. Posner, "Spiky sea clutter at high range resolutions and very low grazing angles," *IEEE Transactions on Aerospace and Electronic Systems*, vol. 38, no. 1, pp. 58–73, 2002.

[4] D. A. Shnidman, "Generalized radar clutter model," *IEEE Transactions on Aerospace and Electronic Systems*, vol. 35, no. 3, pp. 857–865, 1999.

[5] G. Hennessey, H. Leung, A. Drosopoulos, and P. C. Yip, "Sea-clutter modeling using a radial-basis-function neural network," *IEEE Journal of Oceanic Engineering*, vol. 26, no. 3, pp. 358–372, 2001.

[6] N. Xie, H. Leung, and H. Chan, "A multiple-model prediction approach for sea clutter modeling," *IEEE Transactions on Geoscience and Remote Sensing*, vol. 41, no. 6, pp. 1491–1502, 2003.

[7] J. G. Fleischman, S. Ayasli, E. M. Adams, and D. R. Gosselin, "Foliage attenuation and backscatter analysis of SAR imagery," *IEEE Transactions on Aerospace and Electronic Systems*, vol. 32, no. 1, part 3, pp. 135–144, 1996.

[8] J. W. Mccorkle, "Early results from the Army Research Laboratory ultrawide-bandwidth foliage penetration SAR," in *Underground and Obscured Object Imaging and Detection*, vol. 1942 of *Proceedings of SPIE*, Orlando, Fla, USA, April 1993.

[9] D. R. Sheen, N. P. Malinas, D. W. Kletzli, T. B. Lewis, and J. F. Roman, " Foliage transmission measurements using a ground-based ultrawide band (300–1300 MHz) SAR system," *IEEE Transactions on Geoscience and Remote Sensing*, vol. 32, no. 1, pp. 118–130, 1994.

[10] S. Watts, "Radar detection prediction in K-distributed sea clutter and thermal noise," *IEEE Transactions on Aerospace and Electronic Systems*, vol. 23, no. 1, pp. 40–45, 1987.

[11] I. W. Burr, "Cumulative frequency functions," *Annals of Mathematical Statistics*, vol. 13, pp. 215–232, 1942.

[12] P. W. Mielke and E. S. Johnson, "Three-parameter kappa distribution maximum likelihood estimates and likelihood ratio tests," *Monthly Weather Review*, vol. 101, pp. 701–709, 1973.

[13] K. S. Lee, J. Sadeghipour, and J. A. Dracup, "An approach for frequency analysis of multiyear dought duration," *Water Resources Research*, vol. 22, no. 5, pp. 655–662, 1986.

[14] M. M. Shoukri, I. U. H. Mian, and D. S. Tracy, "Sampling properties of estimators of the log-logistic distribution with application to Canadian precipitation data," *The Canadian Journal of Statistics*, vol. 16, no. 3, pp. 223–236, 1988.

[15] N. K. Narda and R. K. Malik, "Dynamic model of root growth and water uptake in wheat," *Journal of Agricultural Engineering*, vol. 3, no. 3-4, pp. 147–155, 1993.

[16] R. C. Gupta, O. Akman, and S. Lvin, "A study of log-logistic model in survival analysis," *Biometrical Journal*, vol. 41, no. 4, pp. 431–443, 1999.

[17] M. Warden, "An experimental study of some clutter characteristics," in *Proceedings of AGARD Conference on Advanced Radar Systems*, May 1970.

[18] G. V. Trunk and S. F. George, "Detection of targets in non-Gaussian sea clutter," *IEEE Transactions on Aerospace and Electronic Systems*, vol. 6, no. 5, pp. 620–628, 1970.

[19] D. C. Schleher, "Radar detection in Weibull clutter," *IEEE Transactions on Aerospace and Electronic Systems*, vol. 12, no. 6, pp. 735–743, 1976.

[20] E. Limpert, W. A. Stahel, and M. Abbt, "Log-normal distributions across the sciences: keys and clues," *BioScience*, vol. 51, no. 5, pp. 341–352, 2001.

[21] W. Weibull, "A statistical distribution function of wide applicability," *Journal of Applied Mechanics*, vol. 18, no. 3, pp. 293–297, 1951.

[22] R. R. Boothe, "The Weibull distribution applied to the ground clutter backscatter coefficient," Tech. Rep. RE-TR-69-15, U.S. Army Missile Command, 1969.

[23] M. Sekine, S. Ohtani, T. Musha, et al., "Weibull-distributed ground clutter," *IEEE Transactions on Aerospace and Electronic Systems*, vol. 17, no. 4, pp. 596–598, 1981.

[24] F. A. Fay, J. Clarke, and R. S. Peters, "Weibull distributed applied to sea clutter," in *Proceedings of the International Radar Conference (Radar '77)*, vol. 155, pp. 101–104, October 1977.

[25] M. Sekine, T. Musha, Y. Tomita, T. Hagisawa, T. Irabu, and E. Kiuchi, "Weibull-distributed sea clutter," *IEE Proceedings F*, vol. 130, no. 5, p. 476, 1983.

[26] M. Sekine, T. Musha, Y. Tomita, T. Hagisawa, T. Irabu, and E. Kiuchi, "On Weibull-distributed weather clutter," *IEEE Transactions on Aerospace and Electronic Systems*, vol. 15, no. 6, pp. 824–830, 1979.

[27] G. A. Tsihrintzis and C. L. Nikias, "Evaluation of fractional, lower-order statistics-based detection algorithms on real radar sea-clutter data," *IEE Proceedings: Radar, Sonar and Navigation*, vol. 144, no. 1, pp. 29–37, 1997.

[28] J. A. Henning, *Design and performance of an ultra-wideband foliage penetrating noise radar*, M.S. thesis, University of Nebraska, May 2001.

[29] J. L. Devore, *Probability and Statistics for Engineering and the Sciences*, BrooksiCole, Monterey, Calif, USA, 1982.

[30] M. Barkat, *Signal Deteciton and Estimation*, Artech House, London, UK, 2nd edition, 2005.

[31] M. A. Richards, *Fundamentals of Radar Signal Processing*, McGraw-Hill, New York, NY, USA, 2005.